the use of Kautz models, which seem to have large potential in many applications in control theory and signal processing, where modeling of resonant systems is of importance.

REFERENCES

[1] P. Lindskog and B. Walhberg, "Applications of Kautz models in system identification," in *IFAC 12th Triennal World Congress*, Sydney, Australia, 1993, pp. 41–44.
[2] B. Wahlberg, "System identification using Kautz models," *IEEE Trans. Automat. Contr.*, vol. 39, pp. 1276–1282, June 1994.
[3] B. Wahlberg and P. M. Mäkilä, "On approximation of stable linear dynamical systems using Laguerre and Kautz functions," *Automatica*, vol. 32, no. 5, pp. 693–708, 1996.
[4] M. A. Masnadi-Shirazi and N. Ahmed, "Laguerre approximation of non recursive discrete-time systems," in *Proc. IEEE Int. Conf. Acoustics, Speech, Signal Processing*, Albuquerque, NM, Apr. 3–6, 1990, pp. 1309–1312.
[5] ——, "Optimum Laguerre networks for a class of discrete-time systems," *IEEE Trans. Signal Processing*, vol. 39, pp. 2104–2108, Sept. 1991.
[6] M. A. Masnadi-Shirazi, "Optimum Synthesis of Linear Discrete-Time Systems Using Orthogonal Laguerre Sequences," Ph.D. dissertation, Univ. New Mexico, Albuquerque, NM, 1990.
[7] T. Oliveira e Silva, "Optimality conditions for truncated Laguerre networks," *IEEE Trans. Signal Processing*, vol. 42, pp. 2528–2530, Sept. 1994.
[8] ——, "On the determination of the optimal pole position of Laguerre filters," *IEEE Trans. Signal Processing*, vol. 43, pp. 2079–2087, Sept. 1995.
[9] ——, "Optimality conditions for truncated Kautz networks with two periodically repeating complex conjugate poles," *IEEE Trans. Automat. Contr.*, vol. 40, pp. 342–346, Feb. 1995.
[10] A. C. Den Brinker, F. P. A. Benders, and T. Oliveira e Silva, "Optimality conditions for truncated Kautz series," *IEEE Trans. Circuits Syst. II*, vol. 43, pp. 117–122, Feb. 1996.
[11] G. J. Clowes, "Choice of the time-scaling factor for linear system approximations using orthonormal Laguerre functions," *IEEE Trans. Automat. Contr.*, vol. AC-10, pp. 487–489, Oct. 1965.
[12] T. W. Parks, "Choice of time scale in Laguerre approximations using signal measurements," *IEEE Trans. Automat. Contr.*, vol. AC-16, pp. 511–513, Oct. 1971.
[13] Y. Fu and G. A. Dumont, "An optimum time scale for discrete Laguerre network," *IEEE Trans. Automat. Contr.*, vol. 38, pp. 934–938, June 1993.
[14] ——, "On determination of Laguerre filter pole through step or impulse response data," in *IFAC 12th Triennal World Congress*, Sydney, Australia, 1993, pp. 35–39.
[15] N. Tanguy, P. Vilbé, and L. C. Calvez, "Optimum choice of free parameter in orthonormal approximations," *IEEE Trans. Automat. Contr.*, vol. 40, pp. 1811–1813, Oct. 1995.
[16] A. C. Den Brinker and H. J. W. Belt, "Optimal free parameters in orthonormal approximations," *IEEE Trans. Signal Processing*, vol. 46, pp. 2081–2087, Aug. 1998.
[17] N. Tanguy, R. Morvan, P. Vilbé, and L. C. Calvez, "Improved method for optimum choice of free parameter in orthogonal approximations," *IEEE Trans. Signal Processing.*, vol. 47, pp. 2576–2579, Sept. 1999.
[18] R. Morvan, N. Tanguy, P. Vilbé, and L. C. Calvez, "Pertinent parameters for Kautz approximation," *Electron. Lett.*, vol. 36, no. 8, pp. 769–771, Apr. 2000.
[19] A. H. G. Gray Jr and J. D. Markel, "A normalized digital filter structure," *IEEE Trans. Acoustics, Speech, Signal Processing*, vol. ASSP-23, pp. 268–277, June 1975.
[20] A. Derrien, "Modélisation des Systèmes Linéaires à Temps Discret via un Procédé D'orthogonalisation et un Algorithme de Gauss-Newton," Ph.D. dissertation, Université de Brest, Brest, France, 1994.

Single State Elastoplastic Friction Models

Pierre Dupont, Vincent Hayward, Brian Armstrong, and Friedhelm Altpeter

Abstract—For control applications involving small displacements and velocities, friction modeling and compensation can be very important. In particular, the modeling of presliding displacement (motion prior to fully developed slip) can play a pivotal role. In this note, it is shown that existing single-state friction models exhibit a nonphysical drift phenomenon which results from modeling presliding as a combination of elastic and plastic displacement. A new class of single state models is defined in which presliding is elastoplastic: under loading, frictional displacement is first purely elastic and then transitions to plastic. The new model class is demonstrated to substantially reduce drift while preserving the favorable properties of existing models (e.g., dissipativity) and to provide a comparable match to experimental data.

Index Terms—Friction compensation, friction modeling, mechanical systems, presliding.

I. INTRODUCTION

Friction modeling is important at all stages of the life cycle of a precision servo. During machine design, accurate friction simulation allows for performance prediction and optimization—suggesting choices of mechanical designs, materials and lubricants to facilitate friction compensation. In compensator design, the role of friction modeling can be categorized according to whether or not the friction compensation is model-based. Examples of nonmodel-based compensators include high-gain feedback [11], impulsive control [3] and dither [7]. These techniques require accurate friction models for analysis: to predict operating point stability [11], limit cycle stability [4] and performance [3]. Model-based compensators perform feedforward cancellation of the friction force. Their success depends on knowledge of the model structure, its observability, and knowledge of the model parameters [8], or, in the case of adaptive controllers, the capability for parameter estimation [2], [13], [18].

The question of appropriate friction models has been raised many times; a 1994 survey cites 280 articles addressing issues of friction modeling, control and applications [5]. Perhaps the most significant impediment to friction modeling is that the physics underlying "sticking" and sliding in lubricated contacts are different. What is classically referred to as "sticking" or static friction is now known to be a regime extending over several microns of motion in metal contacts in which friction force is predominantly a function of displacement [5]. In this regime, known as presliding, friction is a reaction force that compensates for externally applied forces.

In high-precision pointing and tracking applications, presliding can be the dominant friction phenomenon. Dahl, motivated by a coworker's description of the lightly damped relative lateral oscillations of two flat

plates separated by three ball bearings, was the first to attempt to model presliding for controls applications [9]. His model, and a subsequent generalization known as the LuGre model [8], are justified based on their ability to reproduce experimentally observed friction behavior. Dahl's model simulates the symmetric hysteresis loops observed in bearings undergoing small-amplitude sinusoidal forcing. The LuGre model was designed to extend Dahl's model to include other effects, such as those associated with the sliding of lubricated contacts.

Both models incorporate a single continuous state to model presliding displacement. Recently, multi-state models have also been proposed for presliding. As can be expected, they are capable of reproducing more sophisticated presliding behavior—in particular, hysteresis. For example, the model of Swevers *et al.* employs one continuous state plus an array or stack storing positive and negative force/displacement extrema associated with nested hysteresis loops [17].

For many applications, such as machine tools, the single-state models still hold appeal due to their comparative simplicity for system analysis, controller design and implementation. A significant limitation of these models, however, is that they exhibit drift: systems subjected to an arbitrarily small bias force and arbitrarily small vibrations, experience unbounded displacements [15]. For example, the single-state models predict that a block placed in frictional contact with an inclined plane and subjected to small vibrations would creep down the plane. Practical experience shows that this drift is spurious.

In this note, it is shown that drift is due to the fact that presliding displacement in the Dahl and LuGre models always includes a plastic (irreversible) component. To minimize drift, a class of single-state models are defined in which presliding is elastoplastic, i.e., under loading the displacement is first purely elastic (reversible) before transitioning to plastic (irreversible). In Section II, a condition for elastoplastic presliding is defined in terms of a breakaway displacement and a theorem is presented casting this result in terms of single-state model equations. This section also derives conditions on combined elastic and plastic displacement. Sections III presents a new class of single-state models, which are shown to exhibit elastoplastic presliding. In Section IV, machine tool experimental data is used to compare the LuGre and elastoplastic models. Conclusions appear in Section V.

II. SINGLE STATE MODELS

Consider the class of friction models involving a single state variable in which rigid body displacement x is decomposed into elastic (reversible) and plastic (irreversible) components, z and w, respectively

$$x = z + w. \tag{1}$$

Friction models typically define the elastic dynamics explicitly while the plastic displacement w is defined implicitly. For example, Dahl's friction model takes the form

$$f_f = \sigma_0 z, \quad \sigma_0 > 0; \quad \dot{z} = \dot{x}\left(1 - \frac{\sigma_0}{f_C}\mathrm{sgn}(\dot{x})z\right)^i \tag{2}$$

where f_f is the friction force, $z(t)$ specifies the state of elastic strain in the frictional contact, and σ_0, the contact stiffness [9], [10]. With sufficient unidirectional sliding, the force saturates at the Coulomb level f_C. The integer exponent i was used by Dahl to govern the transition rate of z in order to achieve a better experimental match. Applications of his model, however, typically employ the value $i = 1$.

As a second example, the LuGre friction model is an extension of Dahl's model that can provide representations of Stribeck friction, viscous friction, rising static friction and frictional memory during slip [8]. It is written

$$f_f = \sigma_0 z + \sigma_1 \dot{z} + \sigma_2 \dot{x}, \quad \sigma_0, \sigma_1, \sigma_2 > 0;$$
$$\dot{z} = \dot{x}\left(1 - \frac{\sigma_0}{|f_{ss}(\dot{x})|}\mathrm{sgn}(\dot{x})z\right) \tag{3}$$
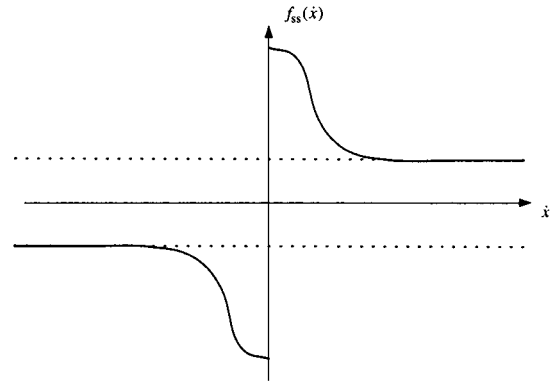

Fig. 1.   Stribeck curve of steady-state friction force versus rigid body velocity $\dot{x}$.

where $f_{ss}(\dot{x})$ is the steady-state friction force versus rigid body velocity, also called the Stribeck curve. A representative plot of f_{ss} versus $\dot{x}$ is seen in Fig. 1. The Stribeck friction curve is sometimes drawn only in the first quadrant; here a more general form is considered in which $f_{ss}(\dot{x})$ is a signed quantity and which allows different values of steady-state friction in the positive and negative motion directions. As before, $z(t)$ specifies the state of elastic strain in the frictional contact; σ_0 and σ_2 are contact stiffness and viscous friction parameters; and σ_1 provides damping for the tangential compliance. The LuGre model specializes to Dahl's model if $\sigma_1 = \sigma_2 = 0$ and $|f_{ss}(\dot{x})| = f_C$.

Introducing the steady-state elastic strain corresponding to steady sliding at velocity $\dot{x}$ as

$$z_{ss}(\dot{x}) = \begin{cases} \frac{f_{ss}(\dot{x})}{\sigma_0}, & |\dot{x}| > 0 \\ \lim_{\dot{x} \to 0^+}\left(\frac{f_{ss}(\dot{x})}{\sigma_0}\right), & \dot{x} = 0 \end{cases} \tag{4}$$

the governing equation of model (3) may be written as

$$\dot{z} = \dot{x}\left(1 - \frac{z}{z_{ss}(\dot{x})}\right) \tag{5}$$

where the second case of $z_{ss}(\dot{x})$ is defined (arbitrarily) to assure that $\dot{z}(\dot{x} = 0) = 0$. For use later in the note, the maximum and minimum steady-state friction values, f_{max} and f_{min}, respectively, are defined as

$$f_{max} = \sup_{\dot{x}}|f_{ss}(\dot{x})| > 0, \tag{6}$$
$$f_{min} = \inf_{\dot{x}}|f_{ss}(\dot{x})| > 0. \tag{7}$$

A. Elastoplastic Presliding

Presliding displacement can be categorized using the rate equations that follow from the displacement equation (1):

$$\left.\begin{array}{r} \dot{x} = \dot{z} \\ \dot{w} = 0 \end{array}\right\} \text{ elastic displacement} \tag{8}$$

$$\dot{x} = \dot{z} + \dot{w} \text{ mixed elastic and plastic displacement} \tag{9}$$

$$\left.\begin{array}{r} \dot{x} = \dot{w} \\ \dot{z} = 0 \end{array}\right\} \text{ plastic displacement/sliding.} \tag{10}$$

The type of presliding displacement provided by a friction model is determined by the sequence of sliding states it produces when subjected to an increasing load from zero initial conditions. The following definitions will be used in this note. *Elastoplastic presliding* starts out elastic (8), proceeds to mixed (9) and then to plastic (10). *Plastic presliding* omits the elastic regime (8) and so always includes a plastic component. A model lacking presliding entirely omits both the elastic and mixed regimes. These observations make it possible to define the requirement for a single-state friction model to exhibit elastoplastic presliding.

Definition 1: A single-state friction model possesses elastoplastic presliding if there exists a breakaway displacement $z_{ba} > 0$ such that $|z(t)| \leq z_{ba}$ implies $\dot{w}(t) = 0, \forall \dot{x} \in \mathbf{R}$.

To apply this definition to single-state friction models, consider the following general equations:

$$f_f = \sigma_0 z + \sigma_1 \dot{z} + \sigma_2 \dot{x}, \quad \sigma_0, \sigma_1, \sigma_2 > 0, \quad (11)$$

$$\dot{z} = \dot{x}\left(1 - \alpha(z, \dot{x})\frac{z}{z_{ss}(\dot{x})}\right). \quad (12)$$

By proper choice of model parameters σ_i and function α, these equations encompass a number of friction models including those of Dahl [9], Haessig and Friedland [14] and the LuGre model [8]. These choices also determine the model's properties as well as the frictional phenomena it can reproduce. The following theorem states the conditions under which a model of this form will exhibit elastoplastic presliding.

Theorem 1: A friction model described by (11) and (12) possesses elastoplastic presliding if and only if there exists a $z_{ba} > 0$ such that $\alpha(z, \dot{x}) = 0, \forall z \in \{|z| \leq z_{ba}\}, \forall \dot{x} \in \mathbf{R}$.

Proof: Assume that the model possesses elastoplastic presliding and is in its elastic regime with $\dot{z} = \dot{x} \neq 0$. By (12), $\alpha(z, \dot{x})[z/z_{ss}(\dot{x})] \equiv 0$. Since $z_{ss}(\dot{x})$ is bounded, this is true if either $z(t) \equiv 0$ or $\alpha(z, \dot{x}) \equiv 0$. However, $z(t) \equiv 0$ contradicts the assumed existence of elastic presliding. Thus, it must be true that $\alpha(z, \dot{x}) = 0$, $\forall z \in \{|z| \leq z_{ba}\}, \forall \dot{x} \in \mathbf{R}$. Now, assume that $\alpha(z, \dot{x}) = 0$, $\forall z \in \{|z| \leq z_{ba}\}, \forall \dot{x} \in \mathbf{R}$. Clearly $\dot{z} = \dot{x}$ and $\dot{w} = 0$ for $|z| \leq z_{ba}$ so that the model possesses elastoplastic presliding. ∎

These results can be used to evaluate the properties of models fitting the form of (11) and (12). For example, casting the LuGre and Dahl models in the form of Theorem 1, they satisfy the inequality

$$0 < \alpha(z, \dot{x})\frac{1}{|z_{ss}(\dot{x})|} < \infty \quad (13)$$

and there is no $z_{ba} > 0$ corresponding to an elastic regime. Thus, with the exception of a constant friction force, $f_f(t) = f_f(t_0), \forall t \geq t_0$, any friction force history produces plastic presliding for these models.

B. Mixed Elastic and Plastic Displacement

Before defining a general elastoplastic model, the cases of elastic displacement combined with either plastic presliding or sliding require a careful description since they define bounds on $\alpha(z, \dot{x})$ in (12). The rate equation governing these combinations is given by (9), and three cases must be considered.

1) Relaxed Contact Undergoing Loading: If a friction model allows a regime of mixed elastic and plastic presliding, a relaxed contact undergoing loading can experience displacement rates satisfying

$$\text{sgn}(\dot{x}) = \text{sgn}(\dot{w}) = \text{sgn}(\dot{z}). \quad (14)$$

This equation constrains the rates of elastic and plastic deformation to fall between the limits obtained in the cases of pure elastic displacement and pure plastic displacement (or equivalently, steady-state sliding). In two special cases, however, one of these equalities can be violated. These are described below.

2) Elastic Relaxation Due to the Stribeck Effect: The Stribeck curve, as depicted in Fig. 1, indicates that the steady-state friction force is a decreasing function of velocity magnitude at low velocities. By (11) and (12), following an increase in velocity, the elastic deformation must decrease, despite continued sliding, to produce the smaller steady-state friction force. The inequality

$$\text{sgn}(\dot{x}) \neq \text{sgn}(\dot{z}) \quad (15)$$

holds during the elastic relaxation. If the friction model includes an elastic damping term, such as $\sigma_1 \dot{z}$ in (11), the elastic damping can reverse the direction of the friction force during relaxation—rendering

the model nondissipative, $f_f \dot{w} < 0$. This effect can be avoided by proper choice of model parameters [1], [6].

3) Elastic "Super Relaxation" Following Motion Reversal: Immediately following a sign change of rigid-body velocity $\dot{x}$, the elastic displacement, z, must relax before stretching in the opposite direction. If the rate of relaxation exceeds the rigid body velocity

$$\text{sgn}(\dot{x}) \neq \text{sgn}(\dot{w}) \quad (16)$$

and dissipation is increased. Given the experimental observation that contacts transitioning to rest from fully developed sliding experience lightly damped tangential oscillations [16], this phenomenon, if present, is of limited effect. It is therefore precluded from the model presented below. However, its inclusion, if needed, is straightforward.

The conditions describing elastic and plastic presliding, as well as sliding, can now be summarized in a time-independent formulation as follows. Equations (8) and (10) yield

$$\frac{dz}{dx} = \begin{cases} 1, & \text{elastic presliding} \\ 0, & \text{plastic presliding/sliding.} \end{cases} \quad (17)$$

Equations (14)–(16) are summarized by

$$\left.\begin{matrix} \text{No Stribeck,} & 0 \\ \text{Stribeck,} & S_{\min} \end{matrix}\right\} \leq \frac{dz}{dx} \leq \begin{cases} 1, & \text{No super relaxation} \\ S_{\max}, & \text{Super relaxation} \end{cases} \quad (18)$$

where the existence of the bounds $S_{\min}$, due to the Stribeck effect, and $S_{\max}$, due to super relaxation, will depend on the equation adopted to describe the dynamics. For the LuGre model and a reasonably smooth Stribeck friction model (e.g., [5]), it is seen from (3) and the fact that $|z| \leq f_{\max}/\sigma_0$ that $S_{\min} = (1 - f_{\max}/f_{\min})$ and $S_{\max} = (1 + f_{\max}/f_{\min})$.

III. THE ELASTO-PLASTIC MODEL

This section presents a class of models of the form of (11) and (12) that exhibit elastoplastic presliding. A breakaway displacement $z_{ba} > 0$ is defined such that the models behave elastically for $|z| < z_{ba}$. This model class also preserves the following properties, which can be achieved by models of the LuGre type. Proofs of these properties are straightforward and can be obtained from [6], [8], and [12].

1) The state z is bounded: If $|z(0)| \leq z_{\max} = f_{\max}/\sigma_0$ then $|z(t)| \leq z_{\max}, \forall t \geq 0$.
2) Equations (17) and (18) are satisfied. Assuming super relaxation is precluded, $0 \leq dz/dx \leq 1$ if no Stribeck effect is modeled and $-\infty < S_{\min} \leq dz/dx \leq 1$, otherwise.
3) During sliding, the friction force opposes slip: $f_f \dot{w} > 0, \forall \dot{w} \neq 0$ (assuming proper choice of model parameters, as discussed in [1], [6]).
4) The model is dissipative for all $\dot{x} \neq 0$.

To achieve these properties, we define the piecewise continuous function $\alpha(z, \dot{x})$:

$$\alpha(z, \dot{x}) = \left.\begin{cases} 0, & |z| \leq z_{ba} \\ \alpha_m(\cdot), & z_{ba} < |z| < z_{ss}(\dot{x}) \\ 1, & |z| \geq z_{ss}(\dot{x}) \\ 0, & \end{cases}\right\} \begin{matrix} \text{sgn}\dot{x} = \text{sgn}z. \\ \\ \text{sgn}\dot{x} \neq \text{sgn}z. \end{matrix} \quad (19)$$

$$\text{with} \quad 0 < z_{ba} \leq z_{ss}(\dot{x}), \quad \forall \dot{x} \in \mathbf{R}. \quad (20)$$
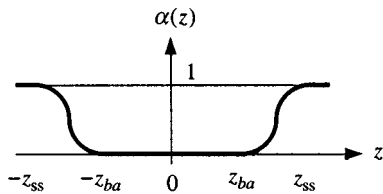
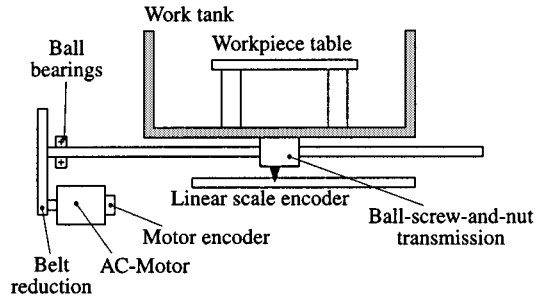Fig. 2. Plot of $\alpha(z, \dot{x})$ for $\mathrm{sgn}(\dot{x}) = \mathrm{sgn}(z)$.

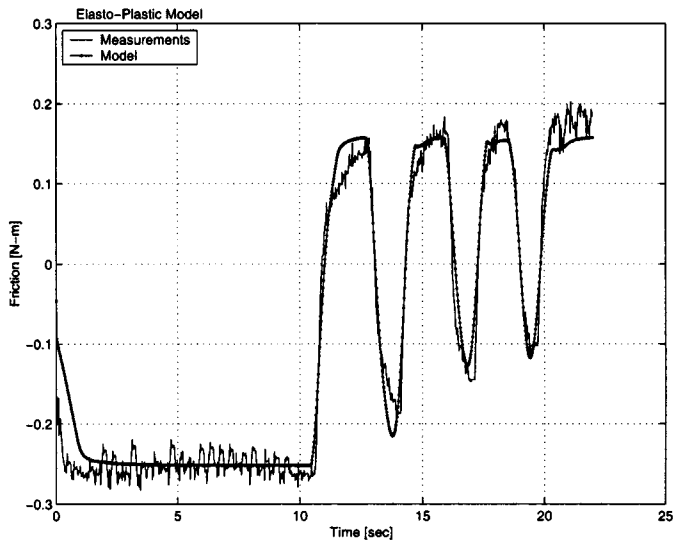Fig. 3. Schematic diagram of electrical discharge machining (EDM) system.

Fig. 4. Friction torque versus time. Both experimental data and elastoplastic model prediction are depicted.

The piecewise continuous function $0 < \alpha_m(\cdot) < 1$ in (19) controls mixed elastic and plastic displacement. A specific example of $\alpha_m(\cdot)$ is given by

$$\alpha_m(z, z_{\mathrm{ba}}, z_{\mathrm{ss}}) = \frac{1}{2} \sin\left(\pi \frac{z - \left(\frac{z_{\mathrm{ss}} + z_{\mathrm{ba}}}{2} \right)}{z_{\mathrm{ss}} - z_{\mathrm{ba}}} \right) + \frac{1}{2},$$

$$z_{\mathrm{ba}} \le |z| < z_{\mathrm{ss}}(\dot{x}). \qquad (21)$$

Graphically, $\alpha(z, \dot{x})$ for $\mathrm{sgn}(\dot{x}) = \mathrm{sgn}(z)$, has the general shape depicted in Fig. 2. The existence of an elastic presliding regime follows directly from (19) and Theorem 1.

The dependence of z_{ss} on $\dot{x}$ is the consequence of forcing the model to represent presliding displacement and the Stribeck effect using just one state. The Stribeck effect describes the steady-state behavior of the separating lubricant film dynamics. The underlying assumption (in common with the LuGre model) is that the fluid layer develops its thickness instantaneously in response to the input $\dot{x}$ and the slower asperity dynamics control the evolution to the steady sliding friction force associated with $\dot{x}$. No attempt is made to justify this assumption here. It is likely that

TABLE I
ESTIMATED FRICTION MODEL PARAMETER VALUES. NOTE THAT FOR THE TRAJECTORIES CONSIDERED, VISCOUS FRICTION IS NEGLIGIBLE, I.E., $\sigma_2 \dot{x} \approx 0$

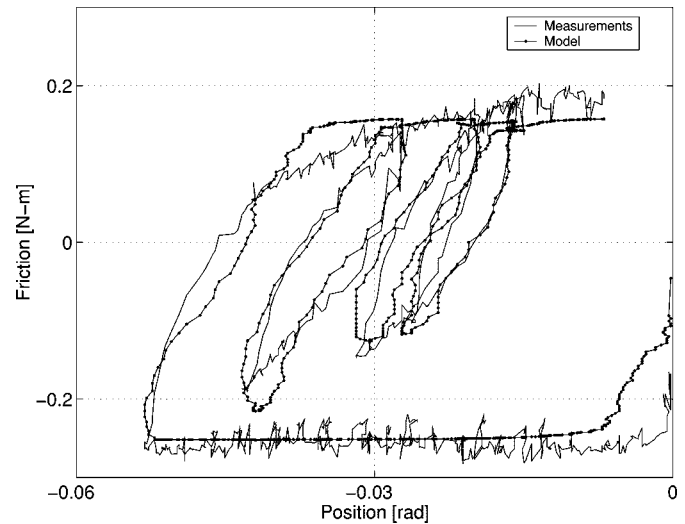| Parameter	Elasto-plastic	LuGre
f_{C} (N-m)	0.2058	0.2345
f_{DC} (N-m)	0.0459	0.0212
$z_{\mathrm{ba}}/z_{\mathrm{ss}}$ (mrad/mrad)	0.7169	NA
σ_0 (N-m/rad)	23.6601	26.3895
σ_1 (N-m-sec/rad)	2.8034	0.8115

Fig. 5. Comparison of friction torque versus angular displacement for measured data and the elastoplastic model.
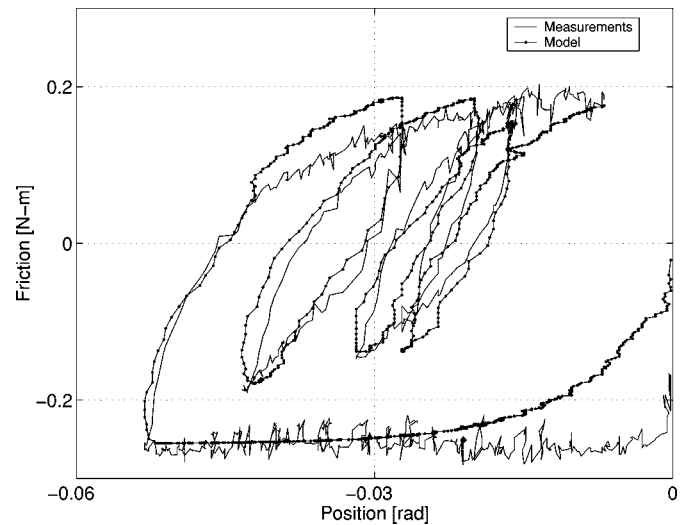

Fig. 6. Comparison of friction torque versus angular displacement for measured data and the LuGre model.

the introduction of additional fluid-related state variables would provide better consistency with the underlying physics. Here, z_{ba} is chosen to be independent of $\dot{x}$. The result is that the range of z over which combined elastic and plastic presliding occurs is a function of $\dot{x}$.

IV. EXPERIMENTAL EVALUATION

To test the capabilities of the elastoplastic model, friction data was obtained from the x-axis of a Charmilles' wire electrical discharge machining (EDM) system. EDM is used to manufacture such items as dies,
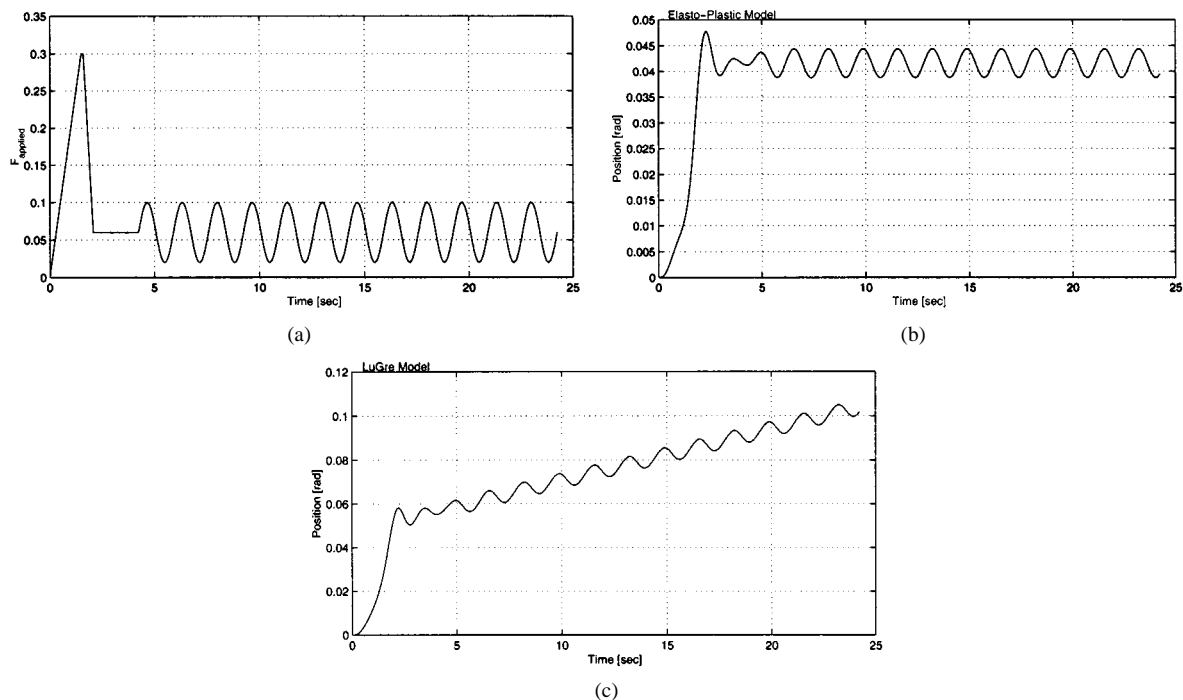
Fig. 7. (a) Motor torque, F_{applied}, versus time. (b) Angular displacement predicted by the elastoplastic friction model. (c) Angular displacement predicted by the LuGre model.

molds and cutting tools. Since the positioning tolerance for these systems is less than a micron, most of the machining operation is performed within friction's presliding regime. With displacement sensing resolution of 0.1 micron becoming the industry standard, these systems provide excellent test beds for measuring the displacement dependence of friction.

A. Test Bed

A schematic diagram of the test machine is shown in Fig. 3. The drive system consists of an ac motor, belt reduction, a ball-screw-and-nut transmission and a linear scale. Friction is primarily present in the various ball bearings and in the transmission system; measurements indicate that linear bearing friction can be assumed negligible. Desired velocity from the machine's CNC is fed to a servo system that controls the AC motor using displacement measurements obtained from both the motor encoder and the linear scale encoder.

For friction parameter estimation, motor encoder position and reference motor torque are sampled at 100 Hz and stored for offline analysis. The belt reduction is extremely stiff; frequency measurements indicate that transmission stiffness exceeds friction interface stiffness by a factor of one hundred. With a transmission reduction ratio of about one thousand, displacements within the presliding regime are easily resolved using the high-resolution motor encoder.

B. Trajectory Design

To design trajectories for estimating presliding friction, preliminary experiments were performed to obtain upper bounds on acceleration and velocity. The bound on acceleration ensured that friction dominated inertia. Thus, friction torque could be estimated using motor current. The bound on velocity ensured that presliding friction dominated viscous friction so that the latter could be neglected. In addition, these machines use boundary lubricants to eliminate the Stribeck effect.

A typical trajectory meeting these requirements is depicted in Fig. 4. It consists of an initial segment of unidirectional sliding, in which a constant friction torque is achieved, followed by seven closely-spaced direction reversals. Such a trajectory tests the capability of a friction

model to reproduce both "major" and "minor" hysteresis loops. Major loops correspond to closed torque-displacement curves, such as those observed by Dahl, in which periodic motion achieves fully developed sliding in both directions. Minor loops are closed torque-displacement curves that occur entirely within presliding.

C. Estimation

Friction parameters were estimated for the elastoplastic and LuGre models by minimizing mean square error in friction force over a trajectory, using a nonlinear search technique. Due to the boundary lubricant, $|f_{\mathrm{ss}}(\dot{x})| = f_C$ is constant for both models. Its value was found to depend on the direction of motion, however, so an offset term, f_{DC}, was introduced. Velocity was estimated from first-order differencing of position data followed by symmetric low-pass filtering at 3 Hz.

Parameter estimates for the elastoplastic model, described by (11), (12), (19)–(21), with $z_{\mathrm{ss}}(\dot{x}) = f_C/\sigma_0$, and the LuGre model, described by (3), are given in Table I. Parameter variances are not provided due to the limited number of trials considered.

Predictions of friction force corresponding to these parameter estimates are shown in Figs. 4 and 5 for the elastoplastic model, and in Fig. 6 for the LuGre model. Estimated friction force is comparable for both models. For the trial depicted, RMS friction error was 11.9% for the elastoplastic model and 12.4% for the LuGre model.

D. Results and Discussion

The advantage of the elastoplastic model is its ability to minimize spurious drift. Its capability to do so is clear from the estimated value $z_{\mathrm{ba}}/z_{\mathrm{ss}} = 0.7169$. This value indicates that for 71.69% of the friction state's range of motion, centered around the unloaded state, presliding displacement is purely elastic. In this range, no drift will occur.

For illustration, consider the motor torque, $F_{\mathrm{applied}}(t)$, shown in Fig. 7(a). Initially, the torque increases linearly so as to exceed the magnitude associated with fully developed (plastic) sliding, $f_C + f_{\mathrm{DC}}$. The torque is then reduced to about one quarter of this level and an oscillatory component is added. Such a component could correspond to system vibration or (position) sensor noise in a feedback loop.
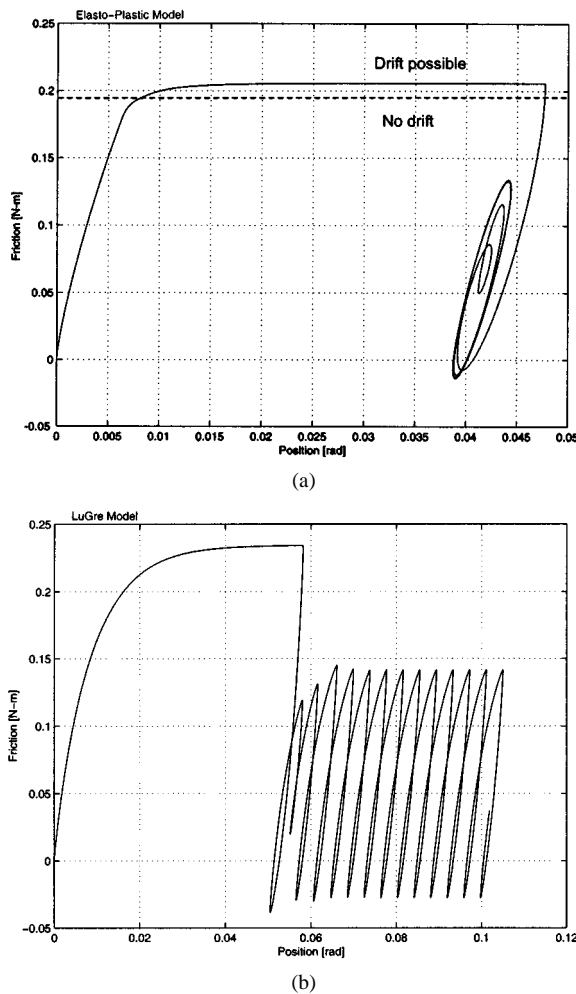
(a)

(b)

Fig. 8. (a) Torque versus displacement for elastoplastic model. The dashed horizontal line is a lower bound on the amplitude of the small loops such that there is no drift. (b) Torque versus displacement for LuGre model. Note the differing horizontal scales.

The response of the EDM machine for this torque input was simulated using the parameter values in Table I. Machine position versus time is plotted in Fig. 7(b) and (c) for the elastoplastic and LuGre models, respectively. The corresponding torque versus displacement curves are shown in Fig. 8(a) and (b). During the initial portion (≈ 2 sec) of the trajectories, both models predict fully developed sliding. This can be most clearly seen by the saturation of the friction forces in Fig. 8.

During the subsequent sinusoidal loading, however, the elastoplastic model predicts elastic presliding with no net displacement. (Note that the area inside the small loops of Fig. 8(a) is due to the damping term $\sigma_1 \dot{z}$ in (11).) The LuGre model, which always includes a plastic component of presliding, predicts that the displacement increases as long as the sinusoidal torque is applied. This drift, which will occur for arbitrarily small sinusoidal torques of the form $F_{\text{applied}} = A + B \sin(\omega t)$; $A, B > 0$, is clearly contrary to the fact that even objects with lubricated contacts remain situated in the presence of small loads and vibrations.

For the elastoplastic model, the quantity $(z_{\text{ba}}/z_{\text{ss}})f_C + f_{\text{DC}} = 0.1934$ N-m, labeled as a dashed horizontal line in Fig. 8(a), provides a lower bound on the torque amplitude $A + B$ for which no drift will occur. Thus, the small loops in this figure can extend at least as high as this boundary without producing any drift. Note that this bound depends on the experimentally estimated ratio $z_{\text{ba}}/z_{\text{ss}}$ and so may vary considerably between applications.

V. CONCLUSION

In high-precision applications, such as EDM, control within the presliding regime is mandatory. Single state models, as approximate representations of friction, are appealing for these applications since their simplicity and continuity facilitate controller design and analysis. Unlike models with many or even infinite states, however, single state models overestimate plastic displacement in presliding—they drift. As demonstrated in Section IV, for applications that involve periodic motions within the presliding regime, the cumulative drift can grow without bound. The elastoplastic models developed in this note eliminate drift in the elastic presliding region and so can substantially reduce total drift. This enhancement can extend the application domain of single state models to trajectories dominated by presliding.

REFERENCES

[1] F. Altpeter, "Friction Modeling, Identification and Compensation," Ph.D. dissertation, Ecole Polytechnique Federale de Lausanne, Lausanne, France, 1999.

[2] F. Altpeter, M. Grunenberg, P. Myszkorowski, and R. Longchamp, "Auto-tuning of feedforward friction compensation based on the gradient method," in *Proc. Amer. Control Conf.*, Chicago, IL, 2000, pp. 2600–2604.

[3] B. Armstrong-Hélouvry, *Control of Machines With Friction*. Boston: Kluwer Academic Press, 1991.

[4] ——, "Stick slip and control in low-speed motion," *IEEE Trans. Automat. Contr.*, vol. 38, pp. 1483–96, Oct. 1993.

[5] B. Armstrong-Hélouvry, P. Dupont, and C. C. De Wit, "A survey of models, analysis tools and compensation methods for the control of machines with friction," *Automatica*, vol. 30, no. 7, pp. 1083–1138, 1994.

[6] N. Barabanov and R. Ortega, "Necessary and sufficient conditions for passivity of the LuGre friction model," *IEEE Trans. Automat. Contr.*, vol. 45, pp. 830–32, Apr. 2000.

[7] J. Bentsman, "Oscillation-induced transitions and their application in control of dynamical systems," *J. Dyna. Syst., Measure. Control*, vol. 112, no. 3, pp. 313–19, 1990.

[8] C. C. de Wit, H. Olsson, and K. Astrôm, "A new model for control of systems with friction," *IEEE Trans. Automat. Contr.*, vol. 40, pp. 419–425, Mar. 1995.

[9] P. Dahl, "A Solid Friction Model," The Aerospace Corporation, El-Segundo, CA, Tech. Rep. TOR-158(3107-18), 1968.

[10] ——, "Solid friction damping of mechanical vibrations," *AIAA J.*, vol. 14, no. 2, pp. 1675–82, 1976.

[11] P. Dupont, "Avoiding stick-slip through PD control," *IEEE Trans. Automat. Contr.*, vol. 39, pp. 1094–1097, May 1994.

[12] P. Dupont, B. Armstrong, and V. Hayward, "Elastoplastic friction model: Contact compliance and stiction," in *Proc. Amer. Control Conf.*, Chicago, IL, 2000, pp. 1072–1077.

[13] N. Leonard and P. Krishnaprasad, "Adaptive friction compensation for bi-directional low-velocity tracking," in *31st Conf. Decision Control*, Tucson, 1992, pp. 267–73.

[14] D. Haessig and B. Friedland, "On the modeling and simulation of friction," *ASME J. Dyna. Syst., Measure. Control*, vol. 113, no. 3, pp. 354–362, 1991.

[15] V. Hayward and B. Armstrong, "A new computational model of friction applied to haptic rendering," in *Experimental Robotics VI*, P. Corke and J. Trevelyan, Eds. Berlin, Germany: Springer-Verlag, 2000, vol. 250, Lecture Notes in Control and Information Sciences, pp. 403–412.

[16] A. Polycarpou and A. Soom, "Transitions between sticking and slipping," in *Proc. Friction Induced Vibration, Chatter, Squeal, Chaos, ASME Winter Annual Meeting*, vol. DE-49, R. A. Ibrahim and A. Soom, Eds., Anaheim, CA, 1992, pp. 139–48.

[17] J. Swevers, F. Al-Bender, C. Ganseman, and T. Prajogo, "An integrated friction model structure with an improved presliding behavior for accurate friction compensation," *IEEE Trans. Automat. Contr.*, vol. 45, pp. 675–86, Apr. 2000.

[18] M. Tomizuka, R. Horowitz, G. Anwar, and Y. Jia, "Implementation of adaptive techniques for motion control of robotic manipulators," *ASME J. Dyna.Syst., Measure. Control*, vol. 110, no. 1, pp. 62–69, 1988.